Computational Materials Science 162 (2019) 314–321

Contents lists available at ScienceDirect

Computational Materials Science

journal homepage: www.elsevier.com/locate/commatsci

Ewald summation for ferroelectric perovksites with charges and dipoles

D. Wang[a,*], J. Liu[b], J. Zhang[a], S. Raza[a], X. Chen[c,d], C.-L. Jia[a,e]

[a] School of Microelectronics & State Key Laboratory for Mechanical Behavior of Materials, Xi'an Jiaotong University, Xi'an 710049, China
[b] State Key Laboratory for Mechanical Behavior of Materials, School of Materials Science and Engineering, Xi'an Jiaotong University, Xi'an 710049, China
[c] Department of Applied Physics, Aalto University, Espoo 00076, Finland
[d] BroadBit Batteries Oy, Espoo 02150, Finland
[e] Peter Grünberg Institute and Ernst Ruska Center for Microscopy and Spectroscopy with Electrons, Research Center Jülich, D-52425 Jülich, Germany

ARTICLE INFO

Keywords:
Ewald method
Perovskite
Coulomb interaction
Effective Hamiltonian

ABSTRACT

Ewald summation is an important technique used to deal with long-range Coulomb interaction. While it is widely used in simulations of molecules and solid state materials, many important results are dispersed in literature and their implementations are often buried deep in large software packages. Since reliable and systematic calculation of Coulomb interaction is critical for the investigation of perovskites, here we start from the fundamentals of Ewald summation and derive clear expressions for long-range charge-charge, dipole-dipole, and charge-dipole interactions, which can be readily used for numerical computations. We also provide the interaction matrix for efficient Monte Carlo simulations involving charges and dipoles, implementing them in a Python software package. A new type of interaction matrix, which accounts for the electrostatic energy change when ions are displaced, is also derived and implemented. These results are the foundations for the investigation of ferroelectric perovskites.

1. Introduction

In the investigation of perovksites, long-range Coulomb interactions are important since they are often the driving force of spontaneous polarization and ferroelectricity [1,2]. Accurate and fast calculations of the dipole-dipole interactions are crucial in such systems [2]. In addition to the dipole-dipole interactions, complex perovksites (e.g., perovskites with doping, alloying, defects, and oxygen vacancy) [3–7] can introduce effective charges and their long-range interactions in perovksites. Therefore, it also becomes inevitable to deal with charge-charge and charge-dipole interactions.

The difficulty to calculate the electrostatic energy in a system with charges and dipoles lies in the long-range nature of Coulomb interaction. The electrostatic energy due to the charge-charge interaction is given by

$$U_{\mathrm{ES}} = \frac{1}{2}\cdot\frac{1}{4\pi\varepsilon_0}\sum_{i,j}\frac{q_i q_j}{|\boldsymbol{r}_i - \boldsymbol{r}_j|}, \tag{1}$$

which decreases slowly with the distance between charges ($\sim 1/r$), making the convergence in numerical computation hard to achieve. In the above expression, $\boldsymbol{r}_i$ is the position of the charge q_i and ε_0 is the vacuum permittivity. In fact, the above series is conditionally convergent, i.e., the result of the sum depends on the order of the terms [8,9]. The justification for using the Ewald method to treat this sum is discussed in Refs. [10,8].

The periodic boundary condition is usually adopted to enable the use of the Ewald method. For infinite and periodic systems, the above expression can be changed by organizing charges into *supercells*

$$U_{\mathrm{ES}} = \frac{1}{2}\left(\frac{1}{4\pi\varepsilon_0}\right)\sum_{\boldsymbol{R_n}}{}'\left(\sum_{i=1}^{N}\sum_{j=1}^{N}\frac{q_i q_j}{|\boldsymbol{r}_{ij} - \boldsymbol{R_n}|}\right) \tag{2}$$

where $\boldsymbol{r}_{ij} \equiv \boldsymbol{r}_i - \boldsymbol{r}_j$, $\boldsymbol{n} = (n_x, n_y, n_z)$ with n_x, n_y, n_z being integers. The summation over i, j is within one supercell containing N charges, and $\boldsymbol{R_n}$ denotes the shift vector to other supercells. By running over all $\boldsymbol{R_n}$, the summation covers all charges in the system by repeating the supercell. The notation $\sum_{\boldsymbol{R_n}}{}'$ signifies that the term where $i = j$ is omitted when $\boldsymbol{R_n} = 0$. The charge at $\boldsymbol{r}_j + \boldsymbol{R_n}$ is often called an image charge of the charge at $\boldsymbol{r}_j$ in the first supercell. In later sections, expressions similar to Eq. (2) will be used.

Straightforward computation of Eq. (1) or Eq. (2) is expensive due to the slow convergence. One solution, which is also the first one of its type, is known as the *Ewald method* introduced in 1921 by Paul P. Ewald [11]. The crucial insight in this approach is to split the sum into two parts, which are treated differently (sum in real and reciprocal spaces) to achieve fast convergence. More specifically, it is necessary to choose

* Corresponding author.
E-mail address: dawei.wang@xjtu.edu.cn (D. Wang).

https://doi.org/10.1016/j.commatsci.2019.03.006
Received 10 January 2019; Received in revised form 1 March 2019; Accepted 1 March 2019

a function $f(r)$ with $r \equiv |\boldsymbol{r}|$ so that

$$\frac{1}{r} = \frac{f(r)}{r} + \frac{1-f(r)}{r}, \tag{3}$$

where $f(r)/r$ shall decay faster with r than $1/r$ (to sum efficiently in real space), while $[1-f(r)]/r$ decays slow in the real space (sum efficiently in the reciprocal space). As we will see below, one choice for $f(r)$ is the *complementary error function*.

The Ewald method is a special type of Poisson solver [12] as it provides the electrostatic potential for a given charge distribution. The Ewald summation is also an application of the more general *Poisson summation* [13]. The formula shown in Eq. (23) is an example of the Poisson summation formula, which is also used in Ref. [14] for systems having periodicity in less than three dimensions.

In an Ewald summation, the reciprocal space is the critical part. In particular, the calculation of terms like $U(\boldsymbol{k})$ in Eq. (27), which represents the charge/dipole distribution in the reciprocal space, needs to be efficiently calculated. In the past, people have tried to optimize the calculation of them, giving rise to the Particle-Particle-Particle-Mesh (P^3M) and Particle-Mesh-Ewald (PME) methods for arbitrary distribution of charges. The main idea is to exploit the Fast Fourier Transformation (FFT) in the evaluation of terms such as Eq. (27). However, given the arbitrary positions of q_i (within a given supercell), an interpolation of the charges to a regular mesh is necessary, which results in the PME method [16]. Another popular method, proposed before PME and also strongly depending on the efficiency of FFT, is the P^3M method [17] which use both the direct sum of particle-particle interaction (for particles close to each other) and the particle-mesh method (to treat particles separated far away). Since provskites already provide us with a regular mesh (thanks to the Bravais lattice), we do not need to use PME or P^3M, but will focus on the interaction matrix [e.g., Eq. (13)], which is necessary for efficient Monte-Carlo (MC) and Molecular Dynamics (MD) simulations of perovskites [2,18–20].

The aim of this work is twofold: (i) Summarize essential results involving Ewald summation dispersed in literature, providing detailed and reliable expressions necessary for numerical implementation. We will cover charge-charge, dipole-dipole, and charge-dipole interactions, needed for understanding complex perovskites with alloying, doping, and defects. Moreover, we also derive the electrostatic energy expression when ions have small displacements (which can induce polarization); (ii) Discuss and provide numerical implementations for each type of interactions mentioned in (i). In particular, we provide Python [21] programs that generate the interaction matrix in the `netcdf` format [22] and consider other less investigated interactions, including the charge-dipole interaction and interactions due to small charge displacements.

In this work, we deal with bulk materials having periodicity in all three dimensions. Ewald summation for finite extent in two or three dimensions is discussed in Refs. [14,23,15]. Such results are necessary for the investigation of nanowires and thin films. It is also worth noting that the Fourier transformation of the dipole interaction matrix can also be accelerated using the Ewald method as discussed in Ref. [24].

This paper is organized as the follows. In Section 2, we treat charge-charge interactions, providing details to explain the Ewald method and preparing for other type of interactions. In Section 3, we obtain the dipole-dipole and dipole-charge interaction matrices. In addition, we also consider how Coulomb energy changes when ions are displaced. In Section 4, we provide information regarding the implementation using Python. In Section 5, we extend the Ewald summation to general Bravais lattices, discuss several less important issues, and provide more details of derivations used in previous sections. Finally in Section 6, we give a brief summary.

2. Charge-charge interaction

We first discuss the charge-charge interaction energy with some details as the results obtained here can serve as starting points for dipole-dipole and charge-dipole interactions. For simplicity, hereafter simple cubic lattice is used with the length of the supercell to be L. General Bravais lattice will be discussed in Section 5.1, which shows a natural transition from the simple cubic lattice is possible. Throughout this paper, we use Latin letters (e.g., i, j) to index charges or dipoles and Greek letters (e.g., α, β) to indicate Cartesian directions (x, y, z). We also use V to denote the volume of the whole crystal and Ω to indicate the volume of the chosen supercell.

2.1. Separated potentials

A key step in the Ewald method is to split the Coulomb interaction into long-range and short-range terms. We first focus on the charge distribution of a point charge q_i at $\boldsymbol{r} = 0$ with the charge distribution

$$\rho_i(\boldsymbol{r}) = \delta(\boldsymbol{r}),$$

which generates a Coulomb potential that slowly decays with $1/r$. Here $\delta(\boldsymbol{r})$ is a Dirac-delta function. The charge distribution can be split into two terms in the following way

$$\rho_i(\boldsymbol{r}) = \rho_i^S(\boldsymbol{r}) + \rho_i^L(\boldsymbol{r}),$$

where

$$\rho_i^S(\boldsymbol{r}) = q_i\delta(\boldsymbol{r}) - q_i G_\sigma(\boldsymbol{r}),$$
$$\rho_i^L(\boldsymbol{r}) = q_i G_\sigma(\boldsymbol{r}),$$

and

$$G_\sigma(\boldsymbol{r}) = \frac{1}{(2\pi\sigma^2)^{3/2}}\exp\left(-\frac{|\boldsymbol{r}|^2}{2\sigma^2}\right),$$

with σ being a constant specifying the spread of the Gaussian function. The physical meaning here is to intentionally introduce a smooth charge distribution that neutralize the point charge at $\boldsymbol{r} = 0$, resulting in $\rho_i^S(\boldsymbol{r})$, which only produces short-range electric potentials (which can be dealt with in real space), and an additional charge distribution $\rho_i^L(\boldsymbol{r})$ (which can be dealt with in the reciprocal space).

The potential field generated by $G_\sigma(\boldsymbol{r})$ can be obtained by solving the Poisson equation,

$$\nabla^2\phi_\sigma(\boldsymbol{r}) = -\frac{G_\sigma(\boldsymbol{r})}{\varepsilon_0}, \tag{4}$$

where the spherical symmetry of $G_\sigma(\boldsymbol{r})$ is used to have

$$\frac{1}{r}\frac{\partial^2}{\partial r^2}(r\phi_\sigma(r)) = -\frac{G_\sigma(\boldsymbol{r})}{\varepsilon_0}.$$

Integration over r gives

$$\frac{\partial}{\partial r}(r\phi_\sigma(r)) = -\int_r^\infty \frac{G_\sigma(r')}{\varepsilon_0}r'dr' = -\frac{\sigma^2}{\varepsilon_0}G_\sigma(r), \tag{5}$$

which results in

$$\phi_\sigma(\boldsymbol{r}) = \frac{1}{4\pi\varepsilon_0 r}\mathrm{erf}\left(\frac{r}{\sqrt{2}\sigma}\right),$$

where $\mathrm{erf}(x) = \frac{2}{\sqrt{\pi}}\int_0^x e^{-\eta^2}d\eta$.

Therefore, the electrostatic potentials generated by $\rho_i^L(\boldsymbol{r})$ and $\rho_i^S(\boldsymbol{r})$ are

$$\phi_i^L(\boldsymbol{r}) = \frac{1}{4\pi\varepsilon_0}\frac{q_i}{|\boldsymbol{r}-\boldsymbol{r}_i|}\mathrm{erf}\left(\frac{|\boldsymbol{r}-\boldsymbol{r}_i|}{\sqrt{2}\sigma}\right), \tag{6}$$

$$\phi_i^S(\boldsymbol{r}) = \frac{1}{4\pi\varepsilon_0}\frac{q_i}{|\boldsymbol{r}-\boldsymbol{r}_i|}\mathrm{erfc}\left(\frac{|\boldsymbol{r}-\boldsymbol{r}_i|}{\sqrt{2}\sigma}\right), \tag{7}$$

where $\mathrm{erf}(x)$ is the error function and $\mathrm{erfc}(x) = 1 - \mathrm{erf}(x)$ is the complementary error function. The three functions $\mathrm{erf}(x)/x$, $\mathrm{erfc}(x)/x$ and $1/x$ are plotted in Fig. 1, which indicates that $\mathrm{erfc}(x)/x$ decays faster

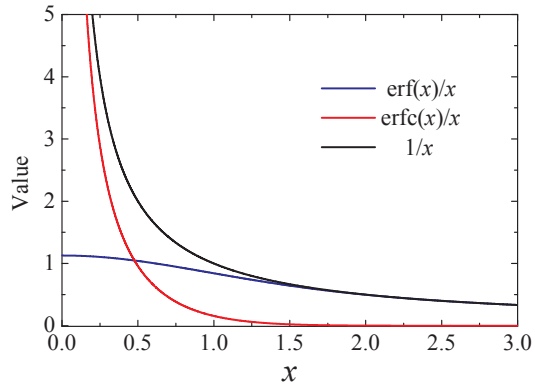

Fig. 1. Comparison of the $\mathrm{erf}(x)/x$, $\mathrm{erfc}(x)/x$, and $1/x$ functions.

than $1/x$ and $\mathrm{erf}(x)/x$ decays similar to $1/x$ for large x.

2.2. E^S and E^L

Given the potentials $\phi_i^S(\boldsymbol{r})$ and $\phi_i^L(\boldsymbol{r})$, the energy can also be split into two parts. Similar to the expression in Eq. (2), the short-range potential due to all charges is given by

$$\begin{aligned}\Phi^S(\boldsymbol{r}) &= \frac{1}{4\pi\varepsilon_0}\sum_{\boldsymbol{n}}\sum_{j=1}^{N} q_j\phi_j(\boldsymbol{r}-\boldsymbol{r}_j-\boldsymbol{n}L)\\ &= \frac{1}{4\pi\varepsilon_0}\sum_{\boldsymbol{n}}\sum_{j=1}^{N}\frac{q_j}{|\boldsymbol{r}-\boldsymbol{r}_j-\boldsymbol{n}L|}\mathrm{erfc}\left(\frac{|\boldsymbol{r}-\boldsymbol{r}_j-\boldsymbol{n}L|}{\sqrt{2}\sigma}\right).\end{aligned}$$

Therefore the electrostatic energy E^S of the system is given by

$$\begin{aligned}E^S &= \frac{1}{2}\sum_{i=1}^{N} q_i\Phi^S(\boldsymbol{r}_i)\\ &= \frac{1}{2}\left(\frac{1}{4\pi\varepsilon_0}\right)\sum_{\boldsymbol{n}}{}'\sum_{i=1}^{N}\sum_{j=1}^{N}\frac{q_iq_j}{|\boldsymbol{r}_i-\boldsymbol{r}_j-\boldsymbol{n}L|}\\ &\quad\times\mathrm{erfc}\left(\frac{|\boldsymbol{r}_i-\boldsymbol{r}_j-\boldsymbol{n}L|}{\sqrt{2}\sigma}\right),\end{aligned}\tag{8}$$

where the overall $1/2$ is necessary to avoid double counting. We note that the above expression is the same as Eq. (2) except the extra factor of $\mathrm{erfc}(|\boldsymbol{r}_i-\boldsymbol{r}_j-\boldsymbol{n}L|/\sqrt{2}\sigma)$. Because $\mathrm{erfc}(x)/x$ decays faster, E^S can be efficiently calculated in real space. In other words, Eq. (8) can be directly used in numerical implementation without further transformation. We also note that Eq. (8) represents the electrostatic energy due to charge-charge interaction within a supercell.

The electrostatic energy due to the long-range potential is given by

$$\begin{aligned}E^L &= \frac{1}{2}\sum_{i=1}^{N} q_i\Phi^L(\boldsymbol{r}_i)\\ &= \frac{1}{2}\frac{1}{4\pi\varepsilon_0}\sum_{\boldsymbol{n}}{}'\sum_{i=1}^{N}\sum_{j=1}^{N}\frac{q_iq_j}{|\boldsymbol{r}_i-\boldsymbol{r}_j-\boldsymbol{n}L|}\\ &\quad\times\mathrm{erf}\left(\frac{|\boldsymbol{r}_i-\boldsymbol{r}_j-\boldsymbol{n}L|}{\sqrt{2}\sigma}\right).\end{aligned}\tag{9}$$

To proceed further (see below), we can use the regular $\sum_n$

$$\begin{aligned}E^L &= \frac{1}{2}\frac{1}{4\pi\varepsilon_0}\sum_{i=1}^{N}\sum_{j=1}^{N} q_iq_j\sum_{\boldsymbol{n}}\frac{q_j}{|\boldsymbol{r}_i-\boldsymbol{r}_j-\boldsymbol{n}L|}\\ &\quad\times\mathrm{erf}\left(\frac{|\boldsymbol{r}_i-\boldsymbol{r}_j-\boldsymbol{n}L|}{\sqrt{2}\sigma}\right)\\ &\quad-\frac{1}{2}\frac{1}{4\pi\varepsilon_0}\sum_{i=1}^{N}\frac{1}{\sigma}\sqrt{\frac{2}{\pi}}q_i^2\end{aligned}\tag{10}$$

where in the last step the relation $\lim_{x\to 0}(\mathrm{erf}(x)/x) = 2/\sqrt{\pi}$ has been used.

Since $\mathrm{erf}(x)/x$ decays slowly ($\sim 1/x$ for large x, see Fig. 1), the expression in Eq. (10) needs to be converted to a sum in the reciprocal space for fast numerical convergence. The core term in Eq. (10) has the form

$$f(\boldsymbol{r}) = \sum_{\boldsymbol{n}}\frac{1}{|\boldsymbol{r}-\boldsymbol{n}L|}\mathrm{erf}\left(\frac{|\boldsymbol{r}-\boldsymbol{n}L|}{\sqrt{2}\sigma}\right),\tag{11}$$

which is periodic as $f(\boldsymbol{r}+\boldsymbol{n}L) = f(\boldsymbol{r})$. Therefore it can be expanded into a Fourier series,

$$f(\boldsymbol{r}) = \sum_{\boldsymbol{k}} a_{\boldsymbol{k}}\exp(i\boldsymbol{k}\cdot\boldsymbol{r}),$$

where $\boldsymbol{k} = 2\pi(m_1, m_2, m_3)/L$ with $m_{1,2,3}$ being integers. We perform the inverse Fourier transformation to have (see Section 5.4 for detailed derivation),

$$a_k = \frac{4\pi}{\Omega k^2}\exp\left(-\frac{k^2\sigma^2}{2}\right),$$

where $\Omega = L^3$ is the volume of the supercell. Therefore, the interaction energy can be represented in the reciprocal space as

$$\begin{aligned}E^L &= \frac{1}{2}\frac{1}{4\pi\varepsilon_0\Omega}\sum_{i=1}^{N}\sum_{j=1}^{N} q_iq_j\sum_{\boldsymbol{k}\neq 0}\frac{4\pi e^{-\sigma^2k^2/2}}{k^2}\cos[\boldsymbol{k}\cdot(\boldsymbol{r}_i-\boldsymbol{r}_j)]\\ &\quad-\frac{1}{4\pi\varepsilon_0}\frac{1}{\sqrt{2\pi}\sigma}\sum_{i=1}^{N} q_i^2.\end{aligned}\tag{12}$$

In the above equation, we have ignored the $\boldsymbol{k} = 0$ term and the reason is explained in Section 5.4.

Finally the total energy due to the charge-charge interaction is given by

$$E_{\mathrm{chg\_chg}} = \sum_{ij}^{N} Q_{ij}q_iq_j,$$

where

$$\begin{aligned}&Q_{ij}\\ &= \frac{1}{2}\frac{1}{4\pi\varepsilon_0}\left\{\frac{1}{|\boldsymbol{r}_i-\boldsymbol{r}_j|}\mathrm{erfc}\left(\frac{|\boldsymbol{r}_i-\boldsymbol{r}_j|}{\sqrt{2}\sigma}\right)(1-\delta_{ij})\right.\\ &\quad+\sum_{n\neq 0}\frac{1}{|\boldsymbol{r}_i-\boldsymbol{r}_j-\boldsymbol{n}L|}\mathrm{erfc}\left(\frac{|\boldsymbol{r}_i-\boldsymbol{r}_j-\boldsymbol{n}L|}{\sqrt{2}\sigma}\right)\\ &\quad\left.+\frac{4\pi}{\Omega}\sum_{\boldsymbol{k}\neq 0}\frac{e^{-\sigma^2k^2/2}}{k^2}\cos[\boldsymbol{k}\cdot(\boldsymbol{r}_i-\boldsymbol{r}_j)]-\frac{1}{\sigma}\sqrt{\frac{2}{\pi}}\delta_{ij}\right\}.\end{aligned}\tag{13}$$

2.3. General result and σ

The derivation shown in Section 2.2 results in a more general expression

$$\begin{aligned}&\sum_n\frac{1}{|\boldsymbol{r}_1-(\boldsymbol{r}_2+\boldsymbol{n}L)|}\\ &=\left[\sum_n\frac{1}{|\boldsymbol{r}_1-\boldsymbol{r}_2-\boldsymbol{n}L|}\mathrm{erfc}\left(\frac{|\boldsymbol{r}_1-\boldsymbol{r}_2-\boldsymbol{n}L|}{\sqrt{2}\sigma}\right)\right.\\ &\quad+\frac{4\pi}{\Omega}\sum_{\boldsymbol{k}\neq 0}\frac{e^{-\sigma^2k^2/2}}{k^2}\cos[\boldsymbol{k}\cdot(\boldsymbol{r}_1-\boldsymbol{r}_2)]\\ &\quad\left.-\lim_{\boldsymbol{r}_i\to\boldsymbol{r}_j}\frac{1}{|\boldsymbol{r}_i-\boldsymbol{r}_j|}\mathrm{erf}\left(\frac{|\boldsymbol{r}_i-\boldsymbol{r}_j|}{\sqrt{2}\sigma}\right)\right].\end{aligned}\tag{14}$$

which can be used in the following sections for the dipole-dipole and dipole-charge interactions. This result is consistent with Ziman's result [25] and will be extended to general Bravais lattice in Section 5.1, where another approach to reach this result is shown.

In principle, the value of σ in Eq. (14) can be chosen arbitrarily. In practice, it shall be chosen to reduce the summation in either the real space or the reciprocal space. It was pointed out that the value of $\alpha = 1/\sqrt{2}\sigma$ can be chosen as $\alpha \approx \sqrt{-\ln\delta}$ so that the error is on the order of δ (e.g., we can set $\delta = 10^{-12}$) [26,27]. We have adopted this choice in our numerical implementations and will show that the real-space summation can be ignored in Section 5.2 [28].

3. Other interaction matrices

The Ewald summation of charge-charge interaction provides us with a basis to derive similar expressions for other types of interactions, such as dipole-dipole and charge-dipole interactions. In obtaining these expressions, point dipoles are assumed. Point dipoles had been employed to numerically simulate perovskites since the introduction of the effective Hamiltonian approach [2], generating many important results and insights. [29,30,19,20,31].

3.1. Dipole-dipole interaction

The dipole-dipole interaction energy in a supercell is given by

$$E_{\text{dip}-\text{dip}}=\frac{1}{2}\frac{1}{4\pi\varepsilon_0}\sum_{i\in\text{supercell}}\sum_{\alpha}(\boldsymbol{u}_i)_\alpha \times\sum_{j\neq i}\sum_{\beta}\left[\frac{\delta_{\alpha,\beta}-3(\hat{\boldsymbol{r}}_{ij})_\alpha(\hat{\boldsymbol{r}}_{ij})_\beta}{r_{ij}^3}\right](\boldsymbol{u}_j)_\beta,$$

where the sum over i is inside the supercell while the sum over j expands to the whole space. Following Eq. (2), the above sum can be further converted to

$$E_{\text{dip}-\text{dip}} =\frac{1}{2}\frac{1}{4\pi\varepsilon_0}{\sum_{\boldsymbol{n}}}'\sum_{i,j}\sum_{\alpha,\beta}(\boldsymbol{u}_i)_\alpha(\boldsymbol{u}_j)_\beta \left[\frac{\delta_{\alpha,\beta}}{|\boldsymbol{r}_{ij}-\boldsymbol{n}L|^3}-\frac{3(\boldsymbol{r}_{ij}-\boldsymbol{n}L)_\alpha(\boldsymbol{r}_{ij}-\boldsymbol{n}L)_\beta}{|\boldsymbol{r}_{ij}-\boldsymbol{n}L|^5}\right],$$

where both i and j belong to the supercell now.

To proceed further, we need to focus on the sum over $\boldsymbol{n}$. For simplicity we use $\boldsymbol{r}=\boldsymbol{r}_i-\boldsymbol{r}_j$ to handle the above expression. A little algebra shows that

$$\sum_n\left[\frac{\delta_{\alpha,\beta}}{|\boldsymbol{r}-\boldsymbol{n}L|^3}-\frac{3(\boldsymbol{r}-\boldsymbol{n}L)_\alpha(\boldsymbol{r}-\boldsymbol{n}L)_\beta}{|\boldsymbol{r}-\boldsymbol{n}L|^5}\right] =-\partial_{r_\alpha}\partial_{r_\beta}\sum_{\boldsymbol{n}}\frac{1}{|\boldsymbol{r}-\boldsymbol{n}L|}. \tag{15}$$

Using the result from Eq. (14) and applying $\partial_{r_\alpha}\partial_{r_\beta}$ to it, we have

$$E_{\text{dip}-\text{dip}} \tag{16}$$
$$=\frac{1}{2}\frac{1}{4\pi\varepsilon_0}\sum_{i,j\in\text{supercell}}\sum_{\alpha,\beta}(\boldsymbol{u}_i)_\alpha(\boldsymbol{u}_j)_\beta \left\{\sum_n\frac{\sqrt{2}}{4\sigma^3x^3}\left[-\delta_{\alpha\beta}B_{\alpha\beta}(x)+\frac{x_\alpha x_\beta}{x^2}C_{\alpha\beta}(x)\right]\Big|_{x=\frac{|\boldsymbol{r}-\boldsymbol{n}L|}{\sqrt{2}\sigma}} +\frac{4\pi}{\Omega}\sum_{\boldsymbol{k}\neq0}\frac{e^{-\sigma^2k^2/2}}{k^2}k_\alpha k_\beta\cos(\boldsymbol{k}\cdot\boldsymbol{r})-\sqrt{\frac{2}{\pi}}\frac{1}{3\sigma^3}\delta_{\alpha\beta}\delta_{ij}\right\},$$

where $x=\frac{|\boldsymbol{r}-\boldsymbol{n}L|}{\sqrt{2}\sigma}$, $B(x)=\frac{2}{\sqrt{\pi}}x\exp(-x^2)+\operatorname{erfc}(x)$, and $C(x)=\frac{2}{\sqrt{\pi}}\left(1+\frac{2x^2}{3}\right)x\exp(-x^2)+\operatorname{erfc}(x)$. For the use in MC simulation, this equation can be rewritten as

$$E_{\text{dip}-\text{dip}}=\sum_{ij,\alpha\beta}^{N}Q_{ij\alpha\beta}(\boldsymbol{u}_i)_\alpha(\boldsymbol{u}_j)_\beta$$

where

$$Q_{ij\alpha\beta}=\frac{1}{2\pi\epsilon_0}\left[\frac{\pi}{\Omega}\sum_{k\neq0}\frac{1}{k^2}e^{-\frac{\sigma^2k^2}{2}} \times\cos(\boldsymbol{k}\cdot\boldsymbol{r}_{ij})k_\alpha k_\beta-\frac{\alpha^3}{3\sqrt{\pi}}\delta_{\alpha\beta}\delta_{ij}\right], \tag{17}$$

same as previous results [2]. In the above expression, the sum in the real space is ignored and the reason is explained in Section 5.2.

3.2. Charge-dipole interaction

Charge-dipole interaction had been discussed in Ref. [32], which has different emphasis than ours. Similar to previous sections, we focus on deriving the interaction matrix. Without the symmetry between charge-charge (or dipole-dipole) interactions, two parts of energy need to be considered, i.e., the energy of charge under the electric potential of dipoles and vice versa. Moreover, to make sure that charges and dipoles are not on exactly the same position, we assume dipoles are on the lattice sites, i.e., $\boldsymbol{r}_i$, while charges are shifted to $\boldsymbol{r}_i+1/2\boldsymbol{a}_1+1/2\boldsymbol{a}_2+1/2\boldsymbol{a}_3$ where $\boldsymbol{a}_{1,2,3}$ are the Bravais lattice. For simple cubic lattice, it is $\boldsymbol{r}_i+(1/2,1/2,1/2)a$ where a is the lattice constant of the unit cell (note L is the lattice constant of the supercell). For simplicity, we use $\boldsymbol{d}$ to denote this shift $\boldsymbol{d}=(1/2,1/2,1/2)a$.

The electrostatic potential given by a dipole $\boldsymbol{u}$ is [33],

$$\phi_i(\boldsymbol{r})=\frac{1}{4\pi\varepsilon_0}\frac{\boldsymbol{u}_i\cdot\boldsymbol{r}}{r^3}=-\frac{\boldsymbol{u}_i}{4\pi\varepsilon_0}\cdot\nabla\left(\frac{1}{\boldsymbol{r}}\right) \tag{18}$$

Therefore, the energy for the charges under dipole potential is given by

$$E_{\text{chg-dip}}=\sum_i\left[-\sum_{\boldsymbol{n}}\sum_j\frac{q_i\boldsymbol{u}_j}{4\pi\varepsilon_0}\cdot\nabla_{\boldsymbol{r}_{ij}}\frac{1}{|\boldsymbol{r}_{ij}+\boldsymbol{d}-\boldsymbol{n}L|}\right]. \tag{19}$$

On the other hand, the potential energy of a dipole in an electric field is given by [33]

$$U=-\boldsymbol{u}\cdot\boldsymbol{E} =\boldsymbol{u}\cdot\nabla\phi(\boldsymbol{r}).$$

Therefore, given the electric field from charges, this energy is

$$E_{\text{dip-chg}}=\sum_j\left[\sum_{\boldsymbol{n}}\sum_i\frac{\boldsymbol{u}_jq_i}{4\pi\varepsilon_0}\cdot\nabla_{\boldsymbol{r}_{ji}}\frac{1}{|\boldsymbol{r}_{ji}-\boldsymbol{d}-\boldsymbol{n}L|}\right] =-\sum_i\left[\sum_{\boldsymbol{n}}\sum_j\frac{\boldsymbol{u}_jq_i}{4\pi\varepsilon_0}\cdot\nabla_{\boldsymbol{r}_{ij}}\frac{1}{|\boldsymbol{r}_{ij}+\boldsymbol{d}-\boldsymbol{n}L|}\right].$$

Hence the total electrostatic energy between charge and dipole is given by

$$E_{\text{CD}}=\frac{1}{2}(E_{\text{dip}-\text{chg}}+E_{\text{dip}-\text{chg}}) =-\sum_{\boldsymbol{n}}\sum_{ij}\frac{q_i\boldsymbol{u}_j}{4\pi\varepsilon_0}\cdot\nabla_{\boldsymbol{r}_{ij}}\left(\frac{1}{|\boldsymbol{r}_{ij}+\boldsymbol{d}-\boldsymbol{n}L|}\right)$$

Following Eq. 14, we obtain

$$\nabla_{\boldsymbol{r}_{ij}}\left(\sum_{\boldsymbol{n}}\frac{1}{|\boldsymbol{r}_{ij}+\boldsymbol{d}-\boldsymbol{n}L|}\right) =\sum_n\left[-\frac{1}{|\boldsymbol{r}_{ij}+\boldsymbol{d}-\boldsymbol{n}L|^2}\operatorname{erfc}\left(\frac{|\boldsymbol{r}_{ij}+\boldsymbol{d}-\boldsymbol{n}L|}{\sqrt{2}\sigma}\right) +\frac{1}{|\boldsymbol{r}_{ij}+\boldsymbol{d}-\boldsymbol{n}L|}\sqrt{\frac{2}{\pi}}\frac{1}{\sigma}\cdot e^{-\left(\frac{|\boldsymbol{r}_{ij}+\boldsymbol{d}-\boldsymbol{n}L|}{\sqrt{2}\sigma}\right)^2}\right] +\frac{4\pi}{\Omega}\sum_{\boldsymbol{k}\neq0}\frac{e^{-\sigma^2k^2/2}}{k^2}\boldsymbol{k}\sin(\boldsymbol{k}\cdot(\boldsymbol{r}_{ij}+\boldsymbol{d})),$$

which leads to

$$E_{\text{CD}}=\sum_{i,j\alpha}^{N}q_iQ_{i,j\alpha}(\boldsymbol{u}_j)_\alpha,$$

where

$$
\begin{aligned}
&Q_{i,j\alpha} \\
&= -\frac{1}{4\pi\varepsilon_0}\Bigg\{\sum_{\boldsymbol{n}}\Bigg[\frac{(\boldsymbol{r}_{ij}+\boldsymbol{d}-\boldsymbol{n}L)_\alpha}{|\boldsymbol{r}_{ij}+\boldsymbol{d}-\boldsymbol{n}L|^3}\mathrm{erfc}\Big(\frac{|\boldsymbol{r}_{ij}+\boldsymbol{d}-\boldsymbol{n}L|}{\sqrt{2}\sigma}\Big) \\
&-\frac{(\boldsymbol{r}_{ij}+\boldsymbol{d}-\boldsymbol{n}L)_\alpha}{|\boldsymbol{r}_{ij}+\boldsymbol{d}-\boldsymbol{n}L|^2}\sqrt{\frac{2}{\pi}}\frac{1}{\sigma}\cdot e^{-\left(\frac{|\boldsymbol{r}_{ij}+\boldsymbol{d}-\boldsymbol{n}L|}{\sqrt{2}\sigma}\right)^2}\Bigg] \\
&-\frac{4\pi}{\Omega}\sum_{\boldsymbol{k}\neq 0}\frac{e^{-\sigma^2k^2/2}}{k^2}\sin[\boldsymbol{k}\cdot(\boldsymbol{r}_{ij}+\boldsymbol{d})]k_\alpha\Bigg\}.
\end{aligned}
\tag{20}
$$

3.3. Ion displacements

Since dipoles arise when charges are displaced from its original positions, one may wonder if it is reasonable to replace dipole-dipole interaction with pure charge-charge interaction in the investigation of perovskites. In this way, the Coulomb energy can be calculated without resorting to dipoles. However, one possible disadvantage will be the recalculation of the Ewald matrix each time when charges are displaced. An alternative way is to implement the P^3M or the PME method in MC programs where particle positions need not be fixed. However, this is likely still too slow since every time one charge is changed, a new computation over the whole system is needed, which necessitates new and more efficient algorithms.

One possible simplification is to deal with small charge displacements. Given the charge-charge interaction matrix, if the charge q_i is displaced by $\boldsymbol{s}_i$ to $\boldsymbol{r}_i - \boldsymbol{n}L + \boldsymbol{s}_i$, the new interaction matrix can be obtained by expanding Q_{ij} to the second order of $\boldsymbol{s}_i$, i.e.,

$$
\begin{aligned}
&Q_{ij}(\{\boldsymbol{r}_i+\boldsymbol{s}_i\}) \\
&= Q_{ij}(\{\boldsymbol{r}_i\}) + \frac{1}{2}\frac{1}{4\pi\varepsilon_0}\Big(-\frac{2\pi}{\Omega}\Big) \\
&\times\sum_{\boldsymbol{k}\neq 0}\frac{e^{-\sigma^2k^2/2}}{k^2}\cos[\boldsymbol{k}\cdot(\boldsymbol{r}_i-\boldsymbol{r}_j)][\boldsymbol{k}\cdot(\boldsymbol{s}_i-\boldsymbol{s}_j)]^2 \\
&= Q_{ij}(\{\boldsymbol{r}_i\}) - \frac{1}{2}\sum_{\alpha\beta}(\boldsymbol{s}_i-\boldsymbol{s}_j)_\alpha(\boldsymbol{s}_i-\boldsymbol{s}_j)_\beta G_{ij\alpha\beta}
\end{aligned}
\tag{21}
$$

where

$$
G_{ij\alpha\beta} = \left(\frac{1}{2\varepsilon_0\Omega}\right)\sum_{\boldsymbol{k}\neq 0}\frac{e^{-\sigma^2k^2/2}}{k^2}\cos[\boldsymbol{k}\cdot(\boldsymbol{r}_i-\boldsymbol{r}_j)]k_\alpha k_\beta. \tag{22}
$$

We note that the expression in Eq. (21) cannot be reduced to the dipole-dipole interaction despite their apparent similarity.

4. Implementation

For calculation involving Ewald summation, there are two common scenarios: (i) Charges and dipoles change frequently and every calculation needs to take into account all the changes. For instance, in a MD simulation all charges and dipoles can change at each time step; and (ii) Only one or just a few charges and dipoles are changed. For instance, in a MC simulation, during one MC sweep the dipoles or charges can be changed individually one by one. For scenario (i), the expressions in Section 5.3 can be useful. For scenario (ii), an interaction matrix can be used to speedup the calculation.

In Sections 2 and 3, we have derived the interaction matrices for charge-charge, dipole-dipole, charge-dipole, displaced charge interactions, which are given in Eqs. (13), (17), (20), and (21), respectively. These matrices are numerically implemented using Python. For computationally intensive parts, we have used C++ to accelerate the calculation [34]. The output of the matrices are stored in `netcdf` format for cross-platform deployment and easy use for different type of simulations (e.g., MC and MD). The source code can be found on `GitLab` [35].

To verify the numerical implementation, we performed a series of tests [35]: (i) For charge-charge interaction matrix, we have used $2\times2\times2$ supercell and calculated the Madelung constants of NaCl ($M = 1.7476$) and CsCl ($M = 1.7627$), obtaining correct results [36]; (ii) We have used $4\times4\times4$ supercell to calculate the dipole-dipole interaction energy (analogy to the Madelung constant) of selected high-symmetry dipole configurations and compared to available results [37] (see Tab. 1); (iii) For charge-dipole interaction matrix, we have constructed a few charge and dipole configurations, calculated the charge-dipole electrostatic energy using the interaction matrix, and compared to the results obtained by direct summation in the real space [38]. These results can be obtained by running the Python programs found in the "test" directory of our `PyEwald` program [35].

Table 1
Dipole interaction for selected high-symmetry dipole configurations.

Symmetry[1]	Ref. [37][2]	Ewald
Γ	$-\frac{2}{3}\pi$	−2.094
X_1	4.844	4.844
X_5	−2.422	−2.422
M_3	−2.677	−2.677
M_5	1.338	1.338
R_{25}	0	-6.348×10^{-10}
Σ_{Lo}	2.932	2.932

[1] The symmetry notations here specify the dipole configurations, which can be found in Ref. [2].

[2] In unit of $Z^*/4\pi\varepsilon_\infty a_0^3$, where Z^* is the effective charge, a_0 is the lattice constant, and ε_∞ is the permittivity.

5. Discussion

Having shown the derivation of main results, we proceed to discuss the applicability of the interaction matrix to general Bravais lattices, the summation in real space, and provide alternative expressions for the total energy and more details important for obtaining results in previous sections.

5.1. General Bravais lattice

In previous sections, simple cubic lattice is conveniently assumed for the Ewald summation. Here let us check if our results can be easily extended to more general Bravais lattice. In the following, we focus on the charge-charge interaction and use it as an example.

The key step here is to check whether Eq. (14) is still valid for general Bravais lattice. To this end, we show that the Poisson-Jacobi relation is also true for general Bravais lattice. That is, we would like to show that the equation

$$
\sum_L e^{-|\boldsymbol{r}+\boldsymbol{L}|^2t^2} = \frac{1}{V}\left(\frac{\pi}{t^2}\right)^{3/2}\sum_k e^{i\boldsymbol{k}\cdot\boldsymbol{r}}\exp\left(-\frac{k^2}{4t^2}\right), \tag{23}
$$

is still valid for a general Bravais lattice. With the previous equation and the fact that

$$
\begin{aligned}
\frac{1}{|\boldsymbol{r}+\boldsymbol{L}_{\boldsymbol{n}}|} &= \frac{2}{\sqrt{\pi}}\int_0^\infty dt\exp(-|\boldsymbol{r}+\boldsymbol{L}_{\boldsymbol{n}}|^2t^2) \\
&= \frac{2}{\sqrt{\pi}}\int_0^\gamma dt\exp(-|\boldsymbol{r}+\boldsymbol{L}_{\boldsymbol{n}}|^2t^2) \\
&+ \frac{2}{\sqrt{\pi}}\int_\gamma^\infty dt\exp(-|\boldsymbol{r}+\boldsymbol{L}_{\boldsymbol{n}}|^2t^2)
\end{aligned}
\tag{24}
$$

the Ewald summation formula can be derived [25,39]. As a matter of fact, these two equations are the basis for an alternative derivation of the Ewald summation adopted by some authors [25]. Therefore, if the Eq. (23) is true for general Bravais lattice, then the expressions of Ewald summation are also true for general Bravais lattice.

In the following, we outline the proof using

$$f(\boldsymbol{r}, t) = \sum_{\boldsymbol{L}_n} e^{-|\boldsymbol{r}+\boldsymbol{L}_n|^2 t^2},$$

where $\boldsymbol{L_n} = \boldsymbol{a}_1 n_1 + \boldsymbol{a}_2 n_2 + \boldsymbol{a}_3 n_3$ and $\boldsymbol{a}_1$, $\boldsymbol{a}_2$ and $\boldsymbol{a}_3$ are the Bravais vectors of a general lattice and $n_{1,2,3}$ are integers. It is easy to see that, $f(\boldsymbol{r} + \boldsymbol{a}_1 n_1 + \boldsymbol{a}_2 n_2 + \boldsymbol{a}_3 n_3, t) = f(\boldsymbol{r}, t)$ is true for arbitrary $n_{1,2,3}$, which shows that $f(\boldsymbol{r}, t)$ is a periodic function that can be expanded into a Fourier series

$$f(\boldsymbol{r}, t) = \sum_m c_m(t) \exp(i\boldsymbol{G}_m \cdot \boldsymbol{r}),$$

with the requirement that $\boldsymbol{G}_m \cdot (\boldsymbol{a}_1 n_1 + \boldsymbol{a}_2 n_2 + \boldsymbol{a}_3 n_3) = 1$ for arbitrary $n_{1,2,3}$. This condition essentially requires that

$$\boldsymbol{G}_m = \boldsymbol{b}_1 m_1 + \boldsymbol{b}_2 m_2 + \boldsymbol{b}_3 m_3,$$

$\boldsymbol{b}_1$, $\boldsymbol{b}_2$ and $\boldsymbol{b}_3$ are the primitive vectors reciprocal to $\boldsymbol{a}_1$, $\boldsymbol{a}_2$ and $\boldsymbol{a}_3$ [25]. The coefficients of the Fourier series are

$$\begin{aligned} c_m(t) &= \frac{1}{V} \sum_{\boldsymbol{L_n}} \int d\boldsymbol{r} e^{-|\boldsymbol{r}+\boldsymbol{L_n}|^2 t^2} \exp(-i\boldsymbol{G}_m \cdot \boldsymbol{r}) \\ &= \frac{1}{\Omega} \int d\boldsymbol{r} e^{-\boldsymbol{r}^2 t^2} \exp(-i\boldsymbol{G}_m \cdot \boldsymbol{r}) \\ &= \frac{1}{\Omega} \left(\frac{\pi}{t^2}\right)^{3/2} \exp\left(-\frac{1}{4t^2} |\boldsymbol{G}_m|^2\right), \end{aligned}$$

where Ω is the volume spanned by $\boldsymbol{a}_1$, $\boldsymbol{a}_2$ and $\boldsymbol{a}_3$.

Therefore

$$\begin{aligned} &\sum_{\boldsymbol{L}_n} e^{-|\boldsymbol{r}+\boldsymbol{L}_n|^2 t^2} \\ &= \frac{1}{\Omega} \left(\frac{\pi}{t^2}\right)^{3/2} \sum_m \exp(i\boldsymbol{G}_m \cdot \boldsymbol{r}) \exp\left(-\frac{1}{4t^2} |\boldsymbol{G}_m|^2\right), \end{aligned} \tag{25}$$

which is the same as Eq. (23) with $\boldsymbol{G}_m$ (made of $\boldsymbol{b}_{1,2,3}$) being the reciprocal lattice of a given general Bravais lattice. Combining the above expression and Eq. (24), we finally have

$$\begin{aligned} &\sum_n \frac{1}{|\boldsymbol{r}+\boldsymbol{L}_n|} \\ &= \frac{4\pi}{\Omega} \sum_m \frac{\exp(-|\boldsymbol{G}_m|^2/4\gamma^2)}{|\boldsymbol{G}_m|^2} \cos(\boldsymbol{G}_m \cdot \boldsymbol{r}) \\ &+ \sum_n \frac{\operatorname{erfc}(|\boldsymbol{r}+\boldsymbol{L}_n| \gamma)}{|\boldsymbol{r}+\boldsymbol{L}_n|}, \end{aligned} \tag{26}$$

which is the the Ewald summation for general Bravais lattices.

The above results indicate that the Ewald method, along with the interaction matrices, can be used for more complex systems other than perovskites. The key procedure to exploy this method is to properly represent all the charges/dipoles in a given system, which can be achieved using a mesh dense enough to hold all charges/dipoles on the lattices. Fig. 2(a) shows the lattice usually chosen to calculate the Madelung constant of NaCl, which is a 2 × 2 × 2 supercell. However, this is not the only choice. Fig. 2(b) shows a finer mesh that gives rise to a 4 × 4 × 4 supercell (note the lattice constant shall be halved to obtain the correct Madelung constant). The second choice will be useful if extra charges/dipoles appear in NaCl (which is unlikely). Following this example, more complex systems can be dealt with in a similar way.

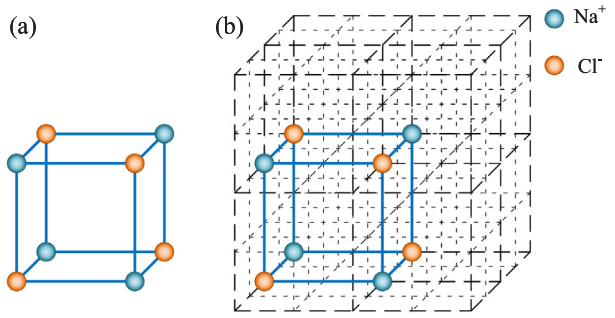

Fig. 2. Different lattices can be chosen to calculate the electrostatic energy of NaCl using the Ewald method (a) a 2 × 2 × 2 supercell and (b) a 4 × 4 × 4 supercell.

5.2. Summation in real space

It can be shown that the real-space summation for all the interaction matrices can be ignored with proper choice of σ. Rather than providing exact proofs, we demonstrate why they can be ignored, which is further verified numerical simulation.

For the charge-charge interaction, we first check the second term of Eq. (13). The largest possible value exists when $\boldsymbol{r}_i = \boldsymbol{r}_j$ and $\boldsymbol{n} = (1, 0, 0)$ or equivalent terms:

$$A = \frac{1}{L} \operatorname{erfc}\left(\frac{L}{\sqrt{2}\sigma}\right) = \frac{1}{L} \operatorname{erfc}(\alpha L).$$

If we choose $\alpha \approx \sqrt{-\ln\delta} = 5.26$ with $\delta = 10^{-12}$ and $L = 1$ (for the smallest $1 \times 1 \times 1$ supercell), then $A = 1.02 \times 10^{-13}$. This value is comparable to the round error in numerical calculation and decreases with L. Using the same argument, it can be shown that the first term can also be safely ignored. Such practice has been numerically verified.

For the dipole-dipole interaction, the real-space sum is more complex as shown in Eq. (16). To estimate how large this term is, we calculate its upper bound

$$\begin{aligned} S(x) &= \frac{1}{\sigma^3 x^3} \sqrt{\sum_{\alpha,\beta} \left[-\delta_{\alpha\beta} B(x) + \frac{3x_\alpha x_\beta}{x^2} C(x)\right]^2} \\ &= \frac{\sqrt{3}}{\sigma^3 x^3} \sqrt{[B(x) - C(x)]^2 + 2C^2(x)} \end{aligned}$$

Since $S(x)$ is a monotonically decreasing function, we can check $|\boldsymbol{r}| = 1$, $\boldsymbol{n} = (0, 0, 0)$ ($x = \frac{|\boldsymbol{r}-\boldsymbol{n}L|}{\sqrt{2}\sigma}$), which gives $S = 9.62 \times 10^{-10}$ when $\alpha = 1/\sqrt{2}\sigma = 5.26$. Therefore it can also be ignored in numerical calculations.

For the charge-dipole interaction, we can again estimate the real-space summation terms in Eq. (20) by calculating the largest terms ($|\boldsymbol{d}| = 0.5$). The value of the two terms are given by

$$\begin{aligned} A &= \frac{1}{d^2} \operatorname{erfc}\left(\frac{d}{\sqrt{2}\sigma}\right) = 4.22 \times 10^{-13}, \\ B &= \frac{1}{d} \sqrt{\frac{2}{\pi}} \frac{1}{\sigma} \exp\left(-\frac{d^2}{2\sigma^2}\right) = 2.37 \times 10^{-11}. \end{aligned}$$

with $\alpha = 1/\sqrt{2}\sigma = 2\sqrt{-\ln(\delta)} = 10.5$. Here the value of α is doubled to compensate the reduced distance (from 1 to 0.5).

5.3. Other useful expressions

In Sections 2, 3.1, and 3.2, we have obtained various interaction matrices that are suitable for simulations when charges and dipoles are changed one by one. There are situations when charges and dipoles are changed by large clusters, where alternative expressions are necessary to further increase the computational efficiency.

The long-range part of the charge-charge interaction in Eq. (12) can be converted to,

$$\begin{aligned} &E^L \\ &= \frac{1}{2} \frac{1}{4\pi\varepsilon_0 \Omega} \sum_{\boldsymbol{k}\neq 0} \frac{4\pi e^{-\sigma^2 k^2/2}}{k^2} |U^2(\boldsymbol{k})| \\ &- \frac{1}{4\pi\varepsilon_0} \frac{1}{\sqrt{2\pi}\sigma} \sum_{i=1}^{N} q_i^2 \end{aligned}$$

where

$$U(\boldsymbol{k}) = \sum_i q_i \exp(i\boldsymbol{k} \cdot \boldsymbol{r}_i). \tag{27}$$

As we have shown in Section 5.2, E^S can be ignored with proper choice of σ. Therefore the above expression is also the total Coulomb energy due to charge-charge interaction.

The dipole energy can be converted to:

$$E_{\text{dip}-\text{dip}}=\frac{1}{2}\frac{1}{4\pi\varepsilon_0}\left(\sqrt{\frac{2}{\pi}}\frac{1}{3\sigma^3}\right)\sum_{i\in\text{supercell}}|\boldsymbol{u}_i|^2 - \frac{1}{2\Omega\varepsilon_0}\sum_{\boldsymbol{k}\neq 0}\frac{e^{-\sigma^2k^2/2}}{k^2}|U(\boldsymbol{k})|^2,$$

where

$$U(\boldsymbol{k})=\sum_i(\boldsymbol{k}\cdot\boldsymbol{u}_i)\exp(i\boldsymbol{k}\cdot\boldsymbol{r}_i),$$

Similarly, the alternative expression for charge-dipole interaction is

$$E^L_{\text{CD}}=-\frac{1}{\Omega\varepsilon_0}\sum_{\boldsymbol{k}\neq 0}\frac{e^{-\sigma^2k^2/2}}{k^2}\Im U(\boldsymbol{k}\cdot\boldsymbol{r}_i+\boldsymbol{k}\cdot\boldsymbol{d})V(\boldsymbol{k}\cdot\boldsymbol{r}_j),$$

where

$$U(\boldsymbol{k})=\sum_i q_i\exp[i(\boldsymbol{k}\cdot\boldsymbol{r}_i+\boldsymbol{k}\cdot\boldsymbol{d})],$$
$$V(\boldsymbol{k})=\sum_j(\boldsymbol{k}\cdot\boldsymbol{u}_j)\exp(i\boldsymbol{k}\cdot\boldsymbol{r}_j),$$

and $\Im$ takes the imaginary part of a complex number.

5.4. Derivation of $a_{\boldsymbol{k}}$

Obtaining the Fourier coefficients of a periodic function as shown in Eq. (3) is important. The coefficient is given by

$$a_{\boldsymbol{k}}=\frac{1}{V}\int_V d\boldsymbol{r}f(r)\exp(-i\boldsymbol{k}\cdot\boldsymbol{r}) =\frac{1}{V}\sum_{\boldsymbol{n}}\int_V d\boldsymbol{r}\frac{1}{|\boldsymbol{r}-\boldsymbol{n}L|}\text{erf}\left(\frac{|\boldsymbol{r}-\boldsymbol{n}L|}{\sqrt{2}\sigma}\right)\exp(-i\boldsymbol{k}\cdot\boldsymbol{r}).$$

Given the periodicity of the function inside the above integral and noting $\boldsymbol{k}$ are the reciprocal lattice points, we have

$$a_{\boldsymbol{k}}=\frac{2\pi}{\Omega}\int_0^\infty dr r\text{erf}\left(\frac{r}{\sqrt{2}\sigma}\right)\int_0^\pi\sin\theta d\theta\exp(-ikr\cos\theta), \tag{28}$$

where spherical coordinate is used and the azimuth axis is set to be along $\boldsymbol{k}$. The above expression can be further converted to

$$a_{\boldsymbol{k}}=\frac{4\pi}{\Omega}\frac{1}{k^2}\int_0^\infty dx\sin x\text{erf}\left(\frac{x}{\sqrt{2}k\sigma}\right) =\frac{4\pi}{\Omega}\frac{1}{k^2}\frac{2}{\sqrt{\pi}}\int_0^\alpha dy\int_0^\infty dx\sin x x\exp(-x^2y^2)$$

where the definition of $\text{erf}(x)$ has been used and $\alpha=1/\sqrt{2}k\sigma$. Integrating over x first we have

$$a_{\boldsymbol{k}}=\frac{2\pi}{\Omega}\frac{1}{k^2}\int_0^\alpha\frac{\exp(-1/4y^2)}{y^3}dy =\frac{4\pi}{\Omega k^2}\exp\left(-\frac{k^2\sigma^2}{2}\right),$$

which is the result we have used in previous sections.

In the above expression, we note that $\boldsymbol{k}=0$ is a special case [33]. From Eq. (28), we have

$$a_0=\frac{4\pi}{\Omega}\int_0^\infty dr r\frac{\sin(kr)}{kr}\Big|_{k=0}\text{erf}\left(\frac{r}{\sqrt{2}\sigma}\right) =\frac{8\pi\sigma^2}{\Omega}\int_0^\infty dx x\text{erf}(x) \equiv\frac{8\pi\sigma^2}{\Omega}X_0$$

where $X_0=\int_0^\infty dx x\text{erf}(x)$ is infinitely large. If this term is included, then the energy of Eq. (12) will be added by one more term, i.e. $\frac{\sigma^2}{\Omega}X_0Q^2$, where $Q=\sum_{i=1}^N q_i$ is the total charge in a supercell. While this term is infinite, if we fix σ, Ω, and assume that the net charge Q in the supercell is a constant (ideally $Q=0$ with charge neutrality), this term becomes a constant that can be ignored in practical calculations concerning energy changes.

6. Summary

To simulate ferroelectric perovskites, the Coulomb potential energy between charges, dipoles, and displaced ions needs to be calculated. For the long-range Coulomb interaction, numerical computation requires the use of the Ewald method. In this work, we have discussed this method in detail, provided interaction matrices, and extended to two less investigated situations: the interaction between charges and dipoles, as well as between displaced ions. In addition, the Ewald method for general Bravais lattice is also considered. We note that, due to the regular distribution of charges or dipoles, the real-space part in the Ewald sum can be ignored. Finally, open source Python programs implementing these interaction matrices are available on GitLab. These analytic results, as well as the computer programs, will find their use in the simulation of ferrelectric materials.

CRediT authorship contribution statement

D. Wang: Conceptualization, Methodology, Software, Writing - original draft. **J. Liu:** Software, Investigation, Writing - original draft, Visualization. **J. Zhang:** Software, Validation. **S. Raza:** Writing - review & editing. **X. Chen:** Methodology, Writing - review & editing. **C.-L. Jia:** Writing - review & editing, Supervision.

Acknowledgement

This work is financially supported by the National Natural Science Foundation of China, Grant No. 11574246, U1537210, and National Basic Research Program of China, Grant No. 2015CB654903. X.C. thanks the financial support from Academy of Finland Projects 308647 and European Union's Horizon2020, Grant No. 760930. D.W. also thanks the support from China Scholarship Council (CSC No. 201706285020).

Data availability

The Python programs are hosted on `GitLab` [35], which are freely available. The accompanying documents to the program can be found at https://dwang5.github.io/PyEwaldDoc/.

References

[1] R.E. Cohen, Origin of ferroeletricity in perovskite oxides, Nature 358 (1992) 136.
[2] W. Zhong, David Vanderbilt, K.M. Rabe, First-principles theory of ferroelectric phase transitions for perovskites: the case of $BaTiO^3$, Phys. Rev. B 52 (1995) 6301.
[3] H.J. Hagemann, D. Hennings, Reversible weight change of acceptor-doped $BaTiO^3$, J. Am. Ceram. Soc. 64 (1981) 590.
[4] Y. Xia, W. He, L. Chen, X. Meng, Z. Liu, Field-induced resistive switching based on space-charge-limited current, Appl. Phys. Lett. 90 (2007) 022907.
[5] W. Hu, Y. Liu, R.L. Withers, T.J. Frankcombe, A. Lasse Norén, M. Snashall, P. Kitchin, B. Smith, H. Gong, J. Chen, F. Brink Schiemer, J. Wong-Leung, Electron-pinned defect-dipoles for high-performance colossal permittivity materials, Nat. Mater. 12 (2013) 821.
[6] H. Tan, Z. Zhao, W.B. Zhu, E.N. Coker, B. Li, M. Zheng, W. Yu, H. Fan, Z. Sun, Oxygen vacancy enhanced photocatalytic activity of pervoskite $SrTiO_3$, ACS Appl. Mater. Interfaces 6 (2014) 19184.
[7] F. Bourguiba, A. Dhahri, F.I.H. Rhouma, S. Mnefgui d, J. Dhahri, K. Taibi, E.K. Hlilet, "Effect of iron and tungsten substitution on the dielectric response and phase transformations of $BaTiO_3$ pervoskite ceramic, J. Alloys Compd. 686 (2016) 675–683.
[8] D. Borwein, J.M. Borwein, K.F. Taylor, Convergence of lattice sums and Madelung's constant, J. Math. Phys. 26 (1985) 2999.
[9] B. Min, Calculation of bulk Madelung constants by direct summation without complications of conditional convergence, J. Korean Phys. Soc. 60 (2012) 1371–1375.
[10] E.S. Campbell, Existence of a well defined specific energy for an ionic crystal; justification of Ewald's formulae and of their use to deduce equations for multipole lattices, J. Phys. Chem. Solids 24 (1963) 197–208.
[11] P. Ewald, Die berechnung optischer und elektrostatischer gitterpotentiale, Ann. Phys. 369 (1921) 253–287.
[12] The Poisson equation concerned here is $\nabla^2\phi=-\rho/\varepsilon$, where ρ is the charge density distribution, ε is the permittivity, and ϕ is the electrostatic potential to be found. Efficient implementation to numerically obtain ϕ is an indispensable part of modern

software packages for density functional theory calculations.
[13] E.M. Stein, R. Shakarchi, Fourier Analysis: An Introduction, Princeton Lectures in Analysis, Princeton University Press, Princeton, 2003.
[14] A. Grzybowski, E. Gwozdz, A. Brodka, Ewald summation of electrstatic interactions in molecular dynamics of a three-dimensional system with periodicity in two directions, Phys. Rev. B 61 (2000) 6706.
[15] A.P. Santos, M. Girotto, Yan Levin, Simulation of Coulomb systems with slab geometry using an efficient 3D Ewald summation method, J. Chem. Phys. 144 (2016) 144103.
[16] T. Darden, D. York, L. Pedersen, Particle mesh Ewald: an $n\log(n)$ method for Ewald sums in large systems, J. Chem. Phys. 98 (1993) 10089.
[17] Roger W. Hockney, James W. Eastwood, Particle-Particle-Particle-Mesh (P3M) Algorithms Computer Simulation using Particles, CRC Press, 1988.
[18] A.R. Akbarzadeh, S. Prosandeev, E.J. Walter, A. Al-Barakaty, L. Bellaiche, Finite-temperature properties of Ba(Zr, Ti)O^3 relaxors from first principles, Phys. Rev. Lett. 108 (2012) 257601.
[19] Z. Jiang, B. Xu, F. Li, D. Wang, C.-L. Jia, Electric dipole sheets in $BaTiO_3/BaZrO_3$ superlattices, Phys. Rev. B 91 (2015) 014105.
[20] D. Wang, A.A. Bokov, Z.-G. Ye, J. Hlinka, L. Bellaiche, Subterahertz dielectric relaxation in lead-free Ba(Zr, Ti)O_3 relaxor ferroelectrics, Nat. Commun. 7 (2016) 11014.
[21] https://www.python.org.
[22] https://www.unidata.ucar.edu/software/netcdf/.
[23] M. Porto, Ewald summation of electrostatic interactions of systems with finite extent in two of three dimensions, J. Phys. A: Math. Gen. 33 (2000) 6211–6218.
[24] G.J. Bowden, R.G. Clark, Fourier transforms of dipole-dipole interactions using Ewald's method, J. Phys. C: Solid State Phys. 14 (1981) L827–L834.
[25] J.M. Ziman, Principles of the Theory of Solids, Cambridge University Press, 1972.
[26] J.W. Perram, H.G. Petersen, S.W. De Leeuw, An algorithm for the simulation of condensed matter which grows as the 3/2 power of the number of particles, Mol. Phys. 65 (1988) 875–893.
[27] A.Y. Toukmaji, J.A. Board Jr., Ewald summation techniques in perspective: a survey, Comp. Phys. Comm. 95 (1996) 73–92.
[28] Note that the unit of σ is length, which is assumed to be 1 in the present work. To deal with the more general case, in our numerical implementation (see Section 4), σ also depends on the lattice constant a (not the length of the supercell L), i.e., $\sigma = a/(\sqrt{-2\ln\delta})$. This choice will ensure that, for any lattice constant, three is no need to include the sum in real space (see Section 5.2; otherwise, for small a, this sum may be necessary).
[29] D. Wang, J. Weerasinghe, A. Albarakati, L. Bellaiche, Terahertz dielectric response and coupled dynamics of ferroelectrics and multiferroics from effective hamiltonian simulations, Int. J. Mod. Phys. B 27 (2013) 1330016.
[30] Z. Jiang, R. Zhang, D. Wang, D. Sichuga, C.-L. Jia, L. Bellaiche, Strain-induced control of domain wall morphology in ultrathin $PbTiO_3$ films, Phys. Rev. B 89 (2014) 214113.
[31] J. Liu, L. Jin, Z. Jiang, L. Liu, L. Himanen, J. Wei, N. Zhang, D. Wang, C.-L. Jia, Understanding doped perovskite ferroelectrics with defective dipole model, J. Chem. Phys. 149 (2018) 244122.
[32] T.L. Beck, Notes on Ewald summation for charges and dipoles (2010).https://homepages.uc.edu/becktl/tlb_ewald.pdf.
[33] J.D. Jackson, Classical Electrodynamics, third ed., John Wiley & Sons, 1999.
[34] https://github.com/pybind/pybind11.
[35] The program is stored on GitLab.https://gitlab.com/dwang5/PyEwald.
[36] Q.C. Johnson, D.H. Templeton, Madelung constants for several structures, J. Chem. Phys. 34 (1961) 2004.
[37] T. Nishimatsu, M. Iwamoto, Y. Kawazoe, U.V. Waghmare, First-principles accurate total energy surfaces for polar structural distortions of $BaTiO_3$, $PbTiO_3$, and $SrTiO_3$: consequences for structural transition temperatures, Phys. Rev. B 82 (2010) 134106.
[38] In one case, we set charges (dipole) with alternating sign (direction) along z. This configuration results in the interaction energy of 4.7173, while direct real-space summation gives 4.727 (the maximum charge-dipole distance d = 100).
[39] M. Mazars, Long ranged interactions in computer simulations and for quasi-2D systems, Phys. Rep. 500 (2011) 43–116.